SBF1 mutations associated with autosomal recessive axonal neuropathy with cranial nerve involvement

Andreea Manole,*[1,2] Alejandro Horga,*[1] Josep Gamez,[3] Nuria Raguer,[4] Maria Salvado,[3] Beatriz San Millán,[5] Carmen Navarro,[5] Alan Pittmann,[2] Mary M. Reilly,[1] Henry Houlden.[1,2]

[1]MRC Centre for Neuromuscular Diseases, UCL Institute of Neurology, Queen Square, London, UK. [2]Department of Molecular Neuroscience, UCL Institute of Neurology, Queen Square, London, United Kingdom. [3]Neuromuscular Disorders Unit, Department of Neurology, Hospital Universitari Vall d'Hebron and Universitat Autònoma de Barcelona, VHIR, Barcelona, Spain. [4]Department of Neurophysiology, Hospital Universitari Vall d'Hebron and Universitat Autònoma de Barcelona, VHIR, Barcelona, Spain. [5]Department of Neuropathology. Complejo Hospitalario Universitario de Vigo, Vigo, Spain.

*These authors contributed equally to the study.

Words in manuscript: 1372

Words in abstract: 95

Number of tables: 1

Number of figures: 1

Number of references: 14

Supplementary material: PDF file

Correspondence to: Dr Josep Gamez. Neuromuscular Disorders Unit, Department of Neurology, Hospital Universitari Vall d'Hebron, Passeig Vall d'Hebron, 119–135, 08035 Barcelona, Spain. Email: josepgamez.bcn@gmail.com. Tel: + 34 932746000. Fax: +34 932110912.

1

ABSTRACT

Biallelic mutations in the *SBF1* gene have been identified in one family with demyelinating Charcot-Marie-Tooth disease (CMT4B3) and two families with axonal neuropathy and additional neurological and skeletal features. Here we describe novel sequence variants in *SBF1* (c.1168C>G and c.2209_2210del) as the potential causative mutations in two siblings with severe axonal neuropathy, hearing loss, facial weakness and bulbar features. Pathogenicity of these variants is supported by co-segregation and *in silico* analyses and evolutionary conservation. Our findings suggest that *SBF1* mutations may cause a syndromic form of autosomal recessive axonal neuropathy (AR-CMT2) in addition to CMT4B3.

ABBREVIATIONS

CMT = Charcot-Marie-Tooth disease; MAF = minor allele frequency.

KEYWORDS

Charcot-Marie-Tooth disease; inherited neuropathy; *MTMR2*; *SBF1*; *SBF2*; whole-exome sequencing.

INTRODUCTION

Charcot-Marie-Tooth disease (CMT), a genetically heterogeneous disorder of the peripheral nerves, is classically divided into demyelinating or axonal subtypes based on neurophysiology data. Mutations in genes encoding myotubularin-related proteins (*MTMR2* and *SBF2*) are associated with autosomal recessive forms of demyelinating CMT (CMT4B1 and CMT4B2, respectively).[1,2] Mutations in the *SBF1* gene, which encodes another member of the myotubularin family, have been identified in one Korean family with autosomal recessive demyelinating CMT (CMT4B3) but also in one Saudi Arabian and one Syrian family with axonal neuropathy, multiple cranial neuropathies, intellectual disability and skeletal features including microcephaly.[3-7] In this paper, we describe novel variants in *SBF1* as the potential causative mutations in two siblings with severe axonal neuropathy, hearing loss, facial weakness and bulbar features. Our findings support the previous observation that *SBF1* mutations may cause a syndromic form of axonal neuropathy in addition to CMT4B3.

METHODS

Two brothers with peripheral neuropathy were investigated. Informed consent was obtained from all individuals and the institutional review boards at the participating medical centres approved the study. Individuals underwent clinical and instrumental assessments during the routine diagnostic process. Neurophysiological studies, MRI scans and skin, muscle and nerve biopsies were performed using standard methods. Genomic DNA from the two affected individuals and four unaffected relatives was used for molecular genetic analyses. For detailed methods see the online supplementary material.

RESULTS

Clinical features. The proband and his affected brother (II:3 and II:2; Fig. 1A) were the third and second children of healthy, non-consanguineous parents of Spanish descent. Both walked independently at age 14 months. At ages 4 and 9 years, respectively, they were noted to have an unsteady gait and subsequently developed slowly progressive, distal-predominant, muscle weakness and sensory loss in their limbs. They lost ambulation in their mid- to late-30s. In their late 40s, on neurological examination, they had gaze-evoked nystagmus (plus delayed initiation of horizontal saccades and mild ophthalmoparesis in patient II:3), bilateral hearing loss, upper and lower facial weakness, bulbar features including tongue weakness, dysarthria, dysphagia and reduced or absent gag reflex, lumbar hyperlordosis, mild pes cavus, distal and proximal muscle weakness and atrophy and marked sensory impairment in their limbs (Table 1 and Fig. 1C-D). They were unable to stand unaided. Their IQ was 85 and 83, respectively.

Nerve conduction studies were consistent with a severe length-dependent, motor and sensory axonal neuropathy with median and ulnar motor nerve conduction velocities ranging between 49 and 61 m/s (supplementary Table 1). Compound muscle action potentials of the facial nerves were markedly reduced in patient II:3. Needle EMG showed neurogenic motor unit action potentials in the limbs and facial muscles (supplementary Table 2). In patient II:3, brainstem auditory evoked potentials were consistent with left sensorineural cochlear impairment and visual evoked potentials showed no abnormalities.

Creatine kinase levels were 290 IU/L in patient II:3 and 420 IU/L in patient II:2 (normal values ≤195 IU/L). Brain MRIs in both cases demonstrated mild cerebellar atrophy (Fig. 1E-F). Skin, tibialis anterior muscle and sural nerve biopsies were performed in patient II:3 at age 34 years. Skin biopsy was unremarkable. Muscle biopsy showed features of longstanding neurogenic atrophy. Nerve biopsy revealed diffuse loss of myelinated axons of all diameters, few regenerating clusters and occasional moderately-thin myelin sheaths; no onion bulbs were observed. The final histopathological diagnosis was axonal neuropathy (Fig. 1G-H). Muscle biopsy of patient II:2 at age 32 years also showed features of longstanding neurogenic atrophy.

Genetic results. Genetic analysis of the 17p11.2 chromosome region and direct sequencing of *GJB1*, *AAAS*, *SLC52A2* and *SLC52A3* genes revealed no pathogenic variants. Genetic tests for spinal muscular atrophy, Kennedy's disease, Friedreich ataxia, spinocerebellar ataxia types 1, 2, 3, 6, 7, 8, 12 and 17, dentatorubral-pallidoluysian atrophy, and fragile X-associated tremor/ataxia syndrome were also negative. To identify the underlying genetic cause, we applied whole-exome sequencing on the proband (II:3) and one unaffected brother (II:1). Analysis focused on nonsynonymous, splice-site and coding indel variants with a minor allele frequency (MAF) of <0.5% in the Exome Aggregation Consortium (ExAC; exac.broadinstitute.org), Exome Variant Server

(EVS; evs.gs.washington.edu) and 1000 Genomes databases (1000G; www.1000genomes.org). From a total of 613 variants that met these filtering criteria in the proband, 186 variants in 60 genes co-segregated under an autosomal recessive model and 2 variants in 2 genes under a X-linked model. Of these 188 variants, only 3 involved a gene associated with inherited neuropathy, i.e. the *SBF1* gene (supplementary Table 3). No potentially pathogenic sequence variants were detected in known genes associated with cerebellar ataxia or hearing loss.

The *SBF1* variants were validated by Sanger sequencing (supplementary Fig.). Segregation analysis confirmed that both affected siblings and their unaffected father were heterozygotes for the *SBF1* variants c.2209_2210del and c.5197C>T, indicating that these two variants were located in the same allele, and that all affected and unaffected siblings and their mother were heterozygous for the *SBF1* variant c.1168C>G (Fig. 1A).

c.2209_2210del and c.1168C>G are novel variants not previously reported in public databases (supplementary Table 4). c.1168C>G, located in exon 11 of the *SBF1* gene (41 exons; Ensembl transcript ENST00000380817), leads to the substitution of positively charged arginine for neutral glycine at codon 390 (p.Arg390Gly), affects a highly conserved nucleotide (Fig. 1B) and amino acid and is predicted as being deleterious by pathogenicity prediction tools. c.2209_2210del, located in exon 19, creates a frame shift starting at codon 737 that ends in a premature stop codon 2 positions downstream (p.Leu737Glufs*3).

c.5197C>T is reported in the dbSNP database (rs199972466) and is present in 62 individuals, including one homozygote, in the ExAC database (MAF = 0.053%; supplementary Table 4). This variant is located in exon 38 and leads to the substitution of positively charged arginine for neutral cysteine at codon 1733 (p.Arg1733Cys). c.5197C>T is predicted as being deleterious; however, in the two affected individuals from the present study, this variant was in *cis* with c.2209_2210del, which causes a premature stop codon 994 amino acids upstream. Thus, the contribution of c.5197C>T to the observed phenotype is uncertain.

DISCUSSION

Using whole-exome sequencing in two siblings with a severe motor and sensory axonal neuropathy, hearing loss, facial weakness and bulbar features we have identified two novel compound heterozygous variants in *SBF1* as the probable causative mutations.

Myotubularins comprise a group of catalytically active and inactive proteins involved in membrane trafficking and endocytosis.[8,9] Inactive myotubularins such as SBF1 and SBF2 interact with and regulate their active homologues by heterodimerization, and coiled-coil domains seem to be crucial for this interaction.[8-10] SBF1 interacts with the MTMR2 lipid phosphatase and deletion of the coiled-coil domain of SBF1 leads to an altered cellular localization of MTMR2 *in vitro*.[10] The frameshift mutation p.Leu737Glufs*3 detected in our family may result in a truncated SBF1 protein lacking the coiled-coil domain, which could affect the activity and distribution of MTMR2. Alternatively, the mutation may cause lack of expression due to nonsense-mediated decay. Of note, nonsense and frameshift mutations are common in *SBF2*-related CMT4B.[2,11,12]

Both SBF1 and SBF2 but not MTMR2 contain DENN domains involved in regulation of Rab GTPases, which are in turn central regulators of membrane trafficking.[13] Mutations affecting the dDENN motif of the DENN domain or nearby amino acid residues have been identified in two families with CMT4B (p.Met417Val in *SBF1* and p.Leu351_Glu432del in *SBF2*) and syndromic forms of axonal neuropathy (p.Leu335Pro and p.Asp443Asn in *SBF1*).[3-7,14] The novel variant p.Arg390Gly detected in our family is also located within the dDENN motif of SBF1, which suggests functional relevance.

Our cases have several similarities with the previously reported Saudi Arabian and Syrian families carrying the homozygous *SBF1* variants p.Asp443Asn and p.Leu335Pro, respectively (clinical features summarized in supplementary Table 5).[4-7] Ophthalmoparesis, facial weakness, dysarthria and dysphagia were present in all families with variable frequency and severity, and neurophysiological exam was consistent with an axonal neuropathy in all individuals although sensory and motor nerve conduction velocities were mildly decreased in one case. Some of the features observed in the previously reported families, however, including strabismus, microcephaly and moderate-to-severe intellectual disability, were absent in our cases. We believe that these three families share a new syndromic form of autosomal recessive axonal neuropathy (AR-CMT2) with multiple cranial neuropathies. Nevertheless, given the phenotypic variability and the previous association of *SBF1*

mutations with CMT4B3, additional studies are needed to further define the clinical spectrum of *SBF1*-related neuropathies.

COMPLIANCE WITH ETHICAL STANDARDS

Ethical approval All procedures performed in studies involving human participants were in accordance with the ethical standards of the institutional and/or national research committee and with the 1964 Helsinki declaration and its later amendments or comparable ethical standards.

Informed consent Informed consent was obtained from all individual participants included in the study. Additional informed consent was obtained from all individual participants for whom identifying information is included in this article.

Conflict of interest The authors declare that they have no conflict of interest.

REFERENCES

1. Bolino A, Muglia M, Conforti FL, et al. Charcot-Marie-Tooth type 4B is caused by mutations in the gene encoding myotubularin-related protein-2 (2000). Nat Genet 25:17–19.

2. Azzedine H, Bolino A, Taieb T, et al. Mutations in MTMR13, a new pseudophosphatase homologue of MTMR2 and Sbf1, in two families with an autosomal recessive demyelinating form of Charcot-Marie-Tooth disease associated with early-onset glaucoma (2003). Am J Hum Genet 72:1141–1153.

3. Nakhro K, Park JM, Hong YB, et al. SET binding factor 1 (SBF1) mutation causes Charcot-Marie-Tooth disease type 4B3 (2013). Neurology 81:165–173.

4. Bohlega S, Alazami AM, Cupler E, Al-Hindi H, Ibrahim E, Alkuraya FS. A novel syndromic form of sensory-motor polyneuropathy is linked to chromosome 22q13.31-q13.33 (2011). Clin Genet 79:193–195.

5. Alazami AM, Alzahrani F, Bohlega S, Alkuraya FS. SET binding factor 1 (SBF1) mutation causes Charcot-Marie-tooth disease type 4B3 (2014). Neurology 82:1665–1666.

6. Mégabarné A, Dorison N, Rodriguez D, Tamraz J. Multiple cranial nerve neuropathies, microcephaly, neurological degeneration, and "fork and bracket sign" in the MRI: a distinct syndrome (2010). Am J Med Genet A 152A: 2297–2300.

7. Romani M, Mehawej C, Mazza T, Mégarbané A, Valente EM. "Fork and bracket" syndrome expands the spectrum of SBF1-related sensory motor polyneuropathies (2016). Neurol Genet 2:e61.

8. Laporte J, Bedez F, Bolino A, Mandel JL. Myotubularins, a large disease-associated family of cooperating catalytically active and inactive phosphoinositides phosphatases (2003). Hum Mol Genet 12:R285–292.

9. Hnia K, Vaccari I, Bolino A, Laporte J. Myotubularin phosphoinositide phosphatases: cellular functions and disease pathophysiology (2012). Trends Mol Med 18:317–327.

10. Kim SA, Vacratsis PO, Firestein R, Cleary ML, Dixon JE. Regulation of myotubularin-related (MTMR)2 phosphatidylinositol phosphatase by MTMR5, a catalytically inactive phosphatase (2003). Proc Natl Acad Sci USA 100:4492–4497.

11. Hirano R, Takashima H, Umehara F, et al. SET binding factor 2 (SBF2) mutation causes CMT4B with juvenile onset glaucoma (2004). Neurology 63:577–580.

12. Baets J, Deconinck T, De Vriendt E, et al. Genetic spectrum of hereditary neuropathies with onset in the first year of life (2011). Brain 134:2664–2676.

13. Marat AL, Dokainish H, McPherson PS. DENN domain proteins: regulators of Rab GTPases (2011). J Biol Chem 286:13791–13800.
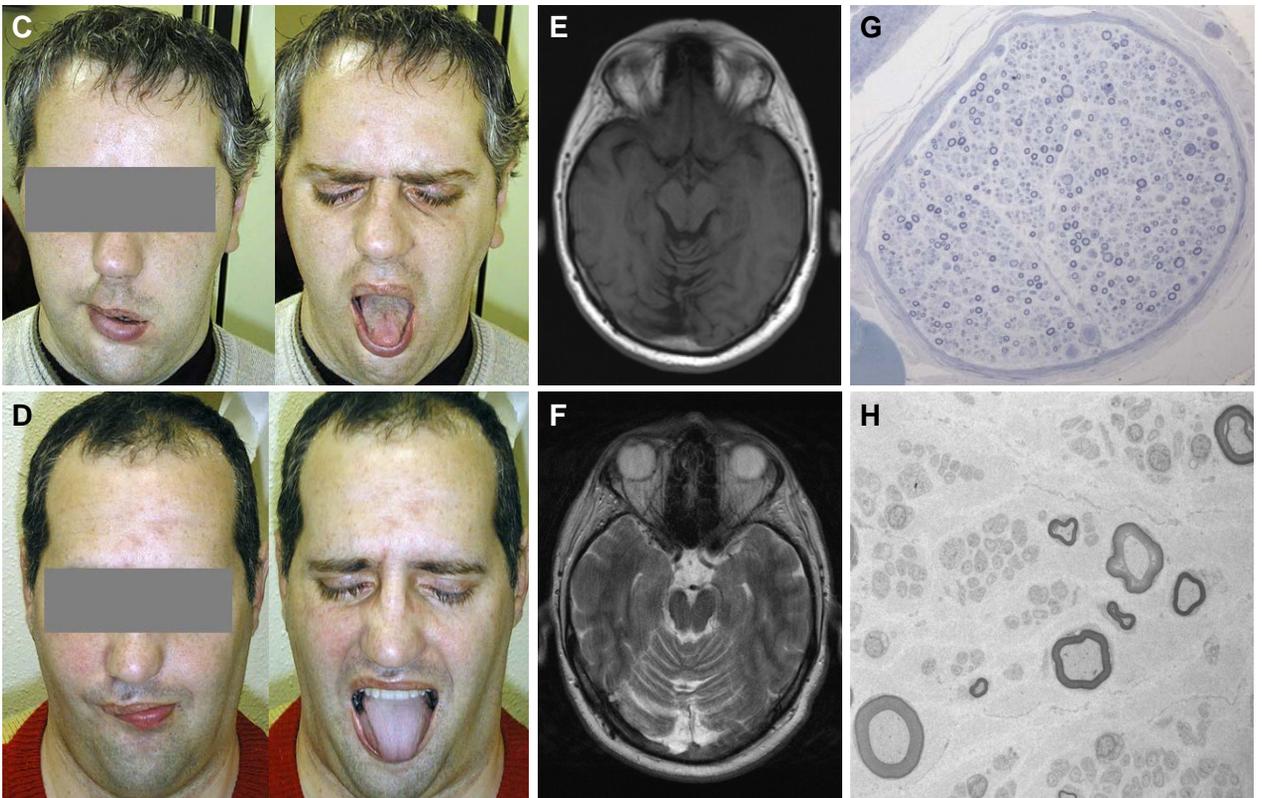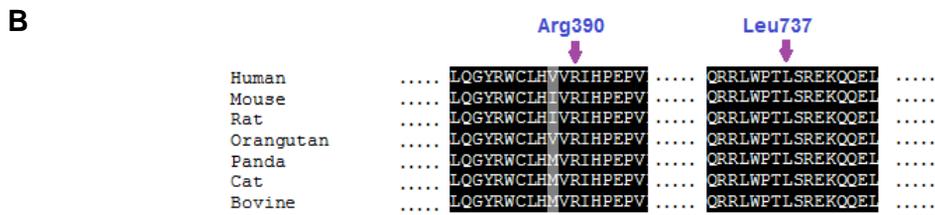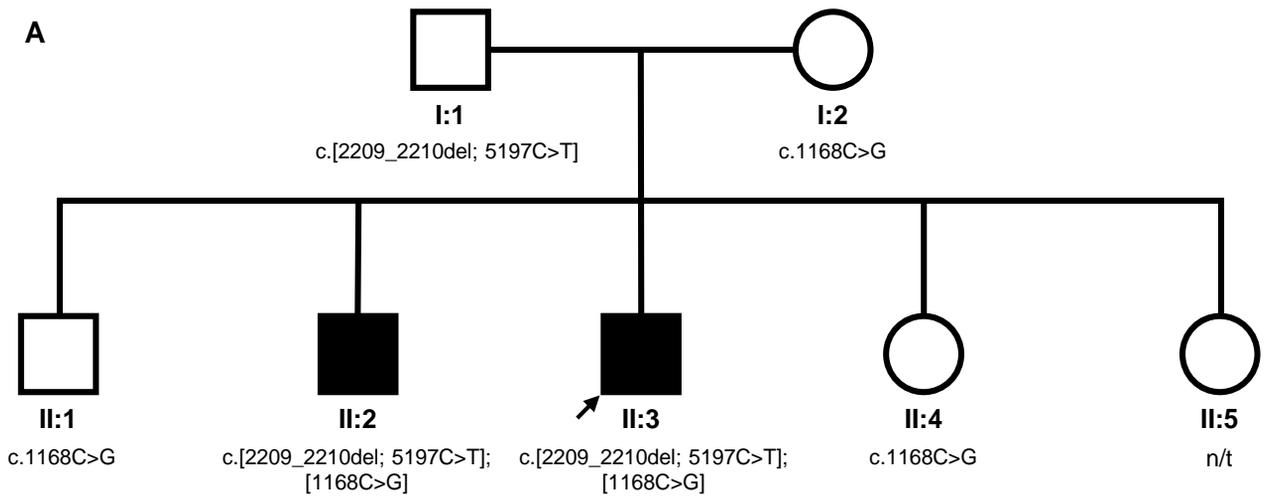
14.   Senderek J, Bergmann C, Weber S, et al. Mutation of the SBF2 gene, encoding a novel member of the myotubularin family, in Charcot-Marie-Tooth neuropathy type 4B2/11p15 (2003). Hum Mol Genet 12:349–356.

Table 1. Clinical features of patients II:3 and II:2.

Patient	II:3	II:2
Gender	Male	Male
Age of onset	4 y	9 y
Age when wheelchair bound	38 y	36 y
Age at examination	48 y	49 y
First symptoms	Gait difficulties	Gait difficulties
Cranial nerves		
Hearing loss	Bilateral	Bilateral
Facial weakness	Bilateral, asymmetric	Bilateral, asymmetric
Ocular movements	Horizontal-gaze evoked nystagmus, delayed initiation of horizontal saccades and ophthalmoparesis	Mild horizontal gaze-evoked nystagmus
Tongue involvement	Weakness	Weakness, atrophy
Dysphagia	Yes	Yes
Dysarthria	Yes	Yes
Gag reflex	Absent	Diminished
Neck flexion	Mild weakness	Mild weakness
Limb involvement		
Muscle tone	Reduced	Reduced
Muscle atrophy	Moderate, distal>proximal	Moderate, distal>proximal
Muscle weakness*		
Upper limb	Distal 3-4 Proximal 3-4 Shoulder abduction 3 Pectoral muscles 3	Distal 2–4 Proximal 3 Shoulder abduction 1 Pectoral muscles 3
Lower limb	No movement except for hip abduction 3	No movement except for knee extension 1-3 and hip abduction 3
Sensory loss		
Pinprick	Reduced to wrists / ankles	Reduced to wrists / ankles
Vibration	Absent to elbows / knees	Absent to elbows / knees
Joint position	Absent at toes	Absent at toes
Deep tendon reflexes	Absent	Absent
Plantar responses	No response	No response
Limb ataxia	Sensory ataxia	Sensory ataxia
Gait pattern	n/e	n/e
Romberg's test	n/e	n/e
Intelligence quotient	85	83
Respiratory involvement	No	Yes, NIV
Other features	Lumbar hyperlordosis Mild pes cavus Gynecomastia	Lumbar hyperlordosis Mild pes cavus Gynecomastia

*Muscle strength according to the Medical Research Council (MRC) grading scale. n/e = not evaluable (unable to perform); NIV = non-invasive ventilation.

Figure 1. (A) Family pedigree and segregation of *SBF1* variants; genotypes are indicated below tested individuals (n/t = not tested). **(B)** Structural conservation of the relevant amino acid residues (Arg390 and Leu737) in *SBF1* across 7 species (single letters = amino acid residues; black = identical; grey = conserved substitution); conservation among species of the affected amino acid residues was determined using Ensembl to retrieve the sequences and ClustalW2 software for multiple sequence alignment. **(C, D)** Clinical images of patients II:2 (C) and II:3 (D) showing asymmetric facial involvement at rest (left images) and incomplete eye closure (right images); note the preserved tongue muscle bulk in patient II:3 and tongue atrophy in patient II:2. **(E, F)** Axial brain MRI images of patient II:2 (T1-weighted image) and patient II:3 (T2-weighted image) showing atrophy of the cerebellar vermis. **(G, H)** Histopathological findings in sural nerve biopsy of patient II:3; transverse semi-thin section (**G**; Toulidine blue stain, magnification x400) and electron micrographs (**H**; original magnification x6200) showing decreased number of myelinated axons of all diameters and occasional moderately-thin myelin sheaths.

A

I:1 c.[2209_2210del; 5197C>T]
I:2 c.1168C>G

II:1 c.1168C>G
II:2 c.[2209_2210del; 5197C>T]; [1168C>G]
II:3 c.[2209_2210del; 5197C>T]; [1168C>G]
II:4 c.1168C>G
II:5 n/t

B

	Arg390	Leu737
Human	LQGYRWCLHVVRIHPEPV	QRRLWPTLSREKQQEL
Mouse	LQGYRWCLHIVRIHPEPV	QRRLWPTLSREKQQEL
Rat	LQGYRWCLHIVRIHPEPV	QRRLWPTLSREKQQEL
Orangutan	LQGYRWCLHVVRIHPEPV	QRRLWPTLSREKQQEL
Panda	LQGYRWCLHMVRIHPEPV	QRRLWPTLSREKQQEL
Cat	LQGYRWCLHMVRIHPEPV	QRRLWPTLSREKQQEL
Bovine	LQGYRWCLHMVRIHPEPV	QRRLWPTLSREKQQEL

C

D

E

F

G

H

SBF1 mutations associated with autosomal recessive axonal neuropathy with cranial nerve involvement

Andreea Manole,*[1,2] Alejandro Horga,*[1] Josep Gamez,[3] Nuria Raguer,[4] Maria Salvado,[3] Beatriz San Millán,[5] Carmen Navarro,[5] Alan Pittmann,[2] Mary M. Reilly,[1] Henry Houlden.[1,2]

[1]MRC Centre for Neuromuscular Diseases, UCL Institute of Neurology, Queen Square, London, UK. [2]Department of Molecular Neuroscience, UCL Institute of Neurology, Queen Square, London, United Kingdom. [3]Neuromuscular Disorders Unit, Department of Neurology, Hospital Universitari Vall d'Hebron and Universitat Autònoma de Barcelona, VHIR, Barcelona, Spain. [4]Department of Neurophysiology, Hospital Universitari Vall d'Hebron and Universitat Autònoma de Barcelona, VHIR, Barcelona, Spain. [5]Department of Neuropathology. Complejo Hospitalario Universitario de Vigo, Vigo, Spain.

*These authors contributed equally to the study.

Correspondence: Dr Josep Gamez. Neuromuscular Disorders Unit, Department of Neurology, Hospital Universitari Vall d'Hebron, Passeig Vall d'Hebron, 119–135, 08035 Barcelona, Spain. Email: josepgamez.bcn@gmail.com.

Supplementary Table 1. Nerve conduction studies of patients II:3 and II:2							
Patient	**II:3**	**II:3**		**II:2**		**II:2**		**Normal**
Age at examination	20 y	48 y		21 y		49 y		**values**
Right / left side	Right	Right	Left	Right	Left	Right	Left	
Motor NCS								
Facial nerve, OO								
DML, ms	-	3.9	4.0	-	-	-	-	≤3.5
D CMAP, mV	-	0.4	0.3	-	-	-	-	≥2.0
Median nerve, APB								
DML, ms	2.6	3.5	-	3.0	-	4.3	-	≤3.9
D/P CMAP, mV	7.2	5.7/5.5	-	9.2	-	8.2/7.0	-	≥3.7
MNCV, m/s	55.3	61.2	-	53.1	-	49	-	≥51
F wave, ms (%)	-	26.1 (20)	-	-	-	NR	-	≤31
Ulnar nerve, ADM								
DML, ms	2.6	3	-	2.7	-	3.6	-	≤3.3
D/P CMAP, mV	5.2	4.2/3.1	-	4.5	-	6.2/5.1	-	≥3.3
MNCV, m/s	60	49.1	-	58.5	-	49.2	-	≥50
F wave, ms (%)	-	28.3 (100)	-	-	-	27.2 (47)	-	≤31
Peroneal nerve, EDB								
DML, ms	5.7	NR	NR	6.1	6.6	NR	5.8	≤6.5
D/P CMAP, mV	2.8	NR	NR	2.5	4.9	NR	0.1/0.1	≥2.5
MNCV, m/s	43.5	NR	NR	41.9	40.1	NR	34.1	≥42
Peroneal nerve, TA								
DML, ms	-	8	-	-	-	5.4	4.8	≤5.0
D CMAP, mV	-	<0.1	-	-	-	<0.1	0.1	≥2
Tibial nerve, TA								
DML, ms	-	9	9.8	-	-	NR	8.4	≤6.0
D/P CMAP, mV	-	<0.1/<0.1	<0.1/<0.1	-	-	NR	<0.1	≥1.8
MNCV, m/s	-	32.6	30.5	-	-	NR	34.5	≥40
Sensory NCS								
Radial nerve								
SNAP, µV	5	4.5	-	-	-	8.2	-	≥15
SNCV, m/s	52	56.1	-	-	-	47.6	-	≥50
Median nerve, D3								
SNAP, µV	7	3	-	10	-	3.1	-	≥7
SNCV, m/s	48.2	50	-	53.8	-	48.3	-	≥46
Ulnar nerve, D5								
SNAP, µV	4	1	-	4	-	3.7	-	≥5
SNCV, m/s	54.5	43.7	-	54.1	-	46	-	≥46
Sural nerve								
SNAP, µV	11	NR	NR	8	9	NR	NR	≥8
SNCV, m/s	42.3	NR	NR	40.5	41.4	NR	NR	≥46

ADM = abductor digiti minimi; AH = abductor hallucis; APB = abductor pollicis brevis; D/P CMAP = distal/proximal compound muscle action potential; D3 = third finger; D5 = fifth finger; DML = distal motor latency; EDB = extensor digitorum brevis; F wave = minimal F wave latency; MNCV = motor nerve conduction velocity; NCS = nerve conduction studies; NR = no response; SNAP = sensory nerve action potential; SNCV = sensory nerve conduction velocity; TA = tibialis anterior; - = not assessed.

Supplementary Table 2. Electromyography results in patients II:3 and II:2

	Spontaneous activity			MUAP morphology			MUAP firing pattern
	Fibrillation potentials	*Positive sharp waves*	*Fascicu-lations*	*Amplitude*	*Polyphasia*	*Duration*	*Recruitment*
Patient II:3 (48 y)							
R Orbicularis oris	1+	1+	0	↑	↑↑	↑	1
R Biceps brachii	2+	2+	0	↑	↑↑	↑	2-3 MUAPs
R Extensor digitorum com.	2+	2+	0	↑	↑	↑	1
R First dorsal interosseous	1+	1+	0	↑	↑	↑	1
R Vastus medialis	0	0	0	-	-	-	0
R Tibialis anterior	1+	1+	0	↑	↑	↑	1 MUAP
R Medial gastrocnemius	0	0	0	↑↑	↑↑	↑	1
Patient II:2 (49 y)							
R Biceps brachii	0	0	0	↑	↑	↑	1
R Extensor digitorum com.	0	0	0	↑	↑	↑	1
R First dorsal interosseous	0	0	0	↑	↑	↑	1
R Rectus femoris	0	0	0	-	-	-	0
R Tibialis anterior	0	0	0	-	-	-	0
R Medial gastrocnemius	0	0	0	↑	↑	↑	1 MUAP

R = right; com = communis; spontaneous activity = 0 none, 1+ mild, 2+ moderate, 3+ many; MUAP = motor unit action potential; MUAP morphology = N normal, ↑ increased, - not evaluable; recruitment = 3 normal, 2 moderately reduced, 1 severely reduced, 0 no recruitment.

Supplementary Table 3. Whole-exome sequencing results and variant filtering.

Individuals	II:3	II:1
Total no. of reads	75,483,464	75,671,510
30x coverage	64.1%	69.1%
20x coverage	80.5%	82.1%
10x coverage	94.3%	93.3%
2x coverage	99.3%	98.6%
Exonic variants	22,828	22,661
Synonymous variants excluded	11,461	11,233
MAF <0.5% (ExAC, EVS and 1000G)	613	132
Rare variants under AR or XL model	188	-
Variants in neuropathy-related genes	3 (*SBF1* gene)	-

AR = autosomal recessive; EVS = Exome Variant Server (http://evs.gs.washington.edu/); ExAC = Exome Aggregation Consortium database (http://exac.broadinstitute.org/); MAF = minor allele frequency; XL = X-linked; 1000G = 1000 Genomes databases (1000G; http://www.1000genomes.org).

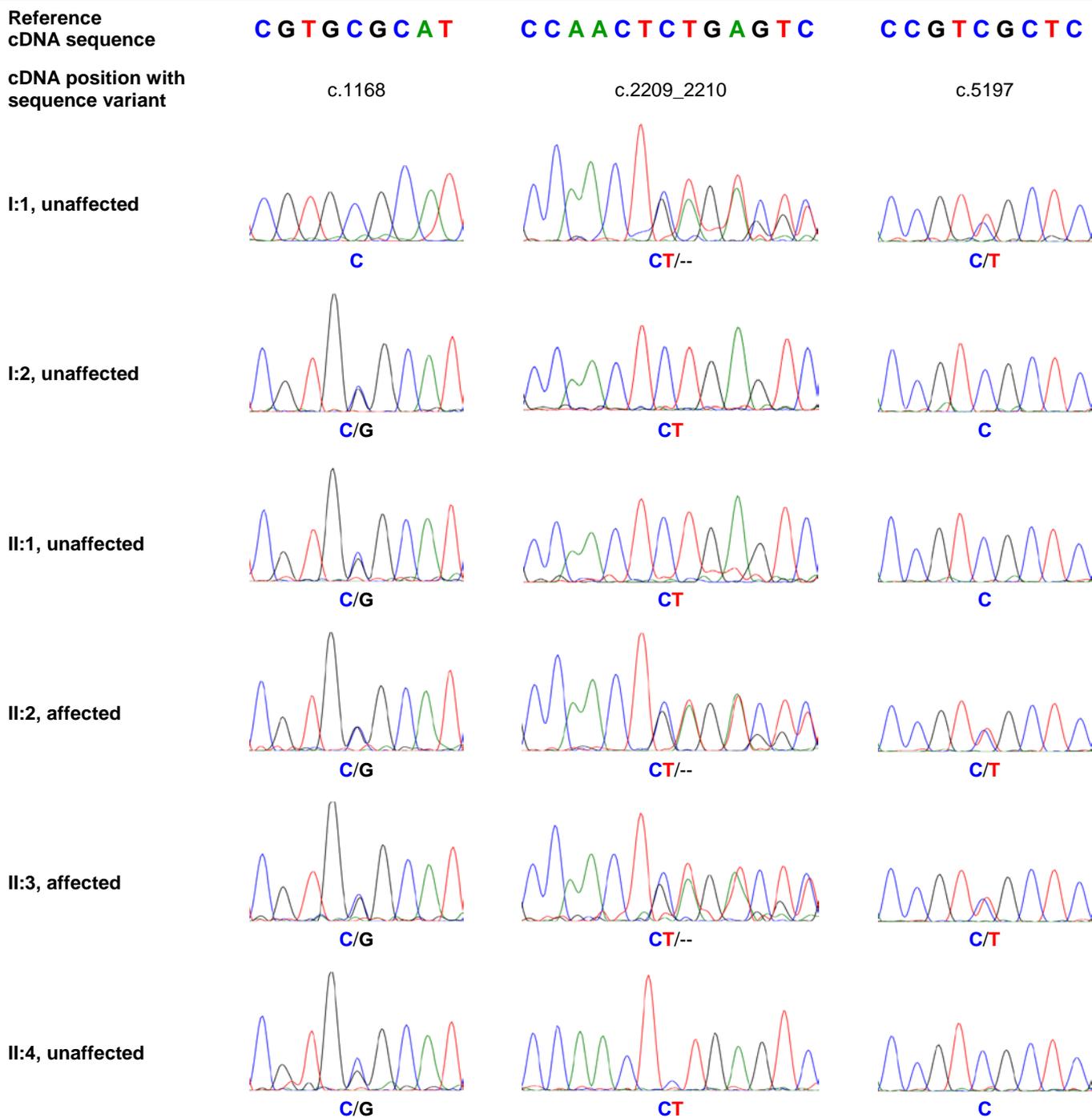| **Supplementary Table 4. Sequence variants in *SBF1*.**			
Chr 22 (GRCh37/hg19)	g.50903679G>C	g.50900820_50900821del	g.50886828G>A
cDNA change	c.1168C>G	c.2209_2210del	c.5197C>T
Protein change	p.Arg390Gly	p.Leu737Glufs*3	p.Arg1733Cys
Exon	11	19	38
rs ID	n/r	n/r	rs199972466
MAF ExAC	n/r	n/r	0.05276%
Grantham	125	-	180
PhyloP	5.47	4.48, 0.176	4.69
GERP	4.49	4.39, -1.78	3.61
SIFT	Deleterious	n/a	Deleterious
PolyPhen2	Probably damaging	n/a	Probably damaging
Mutation Taster	Disease causing	Disease causing	Disease causing

Esembl reference sequences for *SBF1*: ENSG00000100241; ENST00000380817. ExAC = Exome Aggregation Consortium (http://exac.broadinstitute.org/); GERP = Genomic Evolutionary Rate Profiling score (https://genome.ucsc.edu/); Grantham = Grantham Score (supplementary reference 7); MAF = minor allele frequency; Mutation Taster = Mutation Taster v2 (http://www.mutationtaster.org/); PhyloP = PhyloP basewise conservation score derived from multiple sequence alignment of 46 vertebrate species (https://genome.ucsc.edu/); PolyPhen2 = Polymorphism Phenotyping v2 (http://genetics.bwh.harvard.edu/ pph2/); rs ID = reference single nucleotide polymorphism identifier; SIFT = Sorting Intolerant From Tolerant algorithm (http://sift.jcvi.org/); n/r = not reported; n/a = not available.

Supplementary Table 5. Clinical features of patients with syndromic forms of axonal neuropathy due to *SBF1* mutations.

	Present study	Mégarbané 2010, Valente 2016	Bohlega 2011, Alazami 2014
Source	Present study	Mégarbané 2010, Valente 2016	Bohlega 2011, Alazami 2014
Patients	2 siblings	2 siblings	3 siblings
Ethnicity	Spanish	Syrian	Saudi Arabian
SBF1 mutation/s	p.Arg390Gly p.Leu737Glufs*3	p.Leu335Pro homozygous	p.Asp443Asn homozygous
Age of onset	4-9 y	2-7 y	Infancy
First symptoms	Gait difficulties	Microcephaly (2 y), strabismus (4 y), gait difficulties/fatigue (7 y)	Syndactyly, strabismus, cognitive delay, limb weakness (10-20 y)
Hearing loss	Yes	-	-
Nystagmus	Yes	-	-
Strabismus	-	Yes	Yes
Ophthalmoparesis	Yes (1)	Yes	Yes
Absent pupil reactivity	-	Yes	Yes (1)
Facial weakness	Yes	Yes	Yes
Tongue weakness	Yes	-	-
Abnormal gag reflex	Yes	-	Yes (1)
Dysarthria	Yes	Yes	Mild (1)
Dysphagia	Yes	Yes	Yes (1)
Oromandibular dystonia	-	Yes (1)	-
Distal-predominant muscle wasting and weakness	Yes	Yes	Yes
Distal-predominant sensory loss	Yes	-	Yes
Deep tendon reflexes	Absent	Absent	Absent
Foot drop	Yes	Yes (1)	Yes (1)
Pes cavus / planus	Mild pes cavus	Pes cavus	-
Intellectual impairment	IQs 83, 85	Yes	IQs 47, 49, 50
Gynecomastia	Yes	-	-
Microcephaly	-	Yes	Yes
Syndactyly	-	-	Yes
Short stature	-	-	Yes (2)
Lumbar hyperlordosis	Yes	-	-
Elongated face / wide philtrum	-	Yes	-
Mild joint laxity / thumb sign	-	Yes	-
Respiratory involvement	Yes (1)	-	-

Nerve conduction studies and electromyography	Motor and sensory axonal neuropathy	Motor and sensory axonal neuropathy	Motor and sensory axonal neuropathy; mildly reduced CVs (1)
Sural nerve biopsy	Axonal neuropathy (1)	-	Axonal neuropathy (1)
Brain MRI	Mild cerebellar atrophy	Fork and bracket sign; dysplastic left cerebellar cortex (1); brain atrophy (1)	Brain atrophy (2)

The numbers in brackets indicate the number of individuals showing the clinical feature (when lower than the total number of affected individuals).

Supplementary Figure. Sanger sequencing electropherograms and resulting *SBF1* genotypes (Esembl reference sequence ID ENST00000380817).

Reference cDNA sequence	C G T G C G C A T	C C A A C T C T G A G T C	C C G T C G C T C
cDNA position with sequence variant	c.1168	c.2209_2210	c.5197
I:1, unaffected	C	CT/--	C/T
I:2, unaffected	C/G	CT	C
II:1, unaffected	C/G	CT	C
II:2, affected	C/G	CT/--	C/T
II:3, affected	C/G	CT/--	C/T
II:4, unaffected	C/G	CT	C

Supplementary methods

Sanger sequencing. The coding regions and flanking intronic regions of *SBF1* (Ensembl reference sequences: ENSG00000100241; ENST00000380817) were PCR-amplified using PCR Master Mix (Roche). Primer sequences and PCR conditions are shown below. PCR products were cleaned up using the ExoSAP-IT treatment (Affymetrix). Sequencing reactions were performed using Big Dye Terminator v3.1 Cycle Sequencing Kit (Applied Biosystems) and products were purified using the Sephadex G50 filtration kit (Thermo Scientific ABgene). DNA fragments were separated on an ABI3730XL automatic DNA sequencer (Applied Biosystems). The resulting sequences were analysed with SeqScape software v2.5 (Applied Biosystems).

Primer sequences used for PCR and Sanger sequencing of *SBF1* gene		
Exon	**Forward / reverse**	**DNA Sequence**
11	Forward	T T G G G G T G T G G A G A A G C T C
11	Reverse	A T G C G C T T A T C T C C T A C C C C
19	Forward	C T C A T G C G T G T G G T G C C G
19	Reverse	G A A G A A A C T G T G G G C A T G G G
38	Forward	C C A A G T C C C A A C C T C C T G T
38	Reverse	A C C A G T T C G A C A C C C C A A A

PCR protocol		
Temperature (ºC)	**Time (min)**	**Number of cycles**
94	01:00	
94	00:30	
70	00:30	x8
72	00:30	
94	00:30	
70*	00:30	x16
72	00:30	
94	00:30	
65	00:30	x14
72	00:30	
72	05:00	

* Reducing temperature in each cycle

Whole-exome sequencing. The exomes of individuals II:3 and II:1 were enriched using the Nextera Rapid Capture Exome kit (Illumina) and sequenced on the HiSeq 2500 platform (Illumina). The resulting 100 base pairs paired-end sequence reads were mapped against the human reference genome assembly 19 (GRCh37) with the Burrows-Wheeler Aligner package[1] and read duplicates were removed with Picard (http://broadinstitute.github.io/picard/). Variant calling and indel realignments were performed with the Genome Analysis Toolkit (GATK)[2] and variants were submitted to ANNOVAR for annotation.[3]

Bioinformatic analysis. cDNA and protein sequence variants are described in accordance with the recommendations of the Human Genome Variation Society (http://www.hgvs.org) using Ensembl ENSG00000100241; ENST00000380817 as the reference sequences (http://www.ensembl.org/). Evolutionary conservation of nucleotides was assessed using PhyloP (46 vertebrate species) and GERP scores,[4,5] which were accessed through the UCSC Genome Browser (https://genome.ucsc.edu/) using genomic coordinates from GRCh37/hg19. Grantham scores were used to assess the physicochemical nature of the amino acid substitutions.[6] *In silico* analyses of sequence variants were performed using the following pathogenicity prediction tools: SIFT (http://sift.jcvi.org/),[7] PolyPhen-2 (http://genetics.bwh.harvard.edu/ pph2/)[8] and Mutation Taster version 2 (http://www.mutationtaster.org/).[9]

Supplementary references

1. Li H, Durbin R. Fast and accurate short read alignment with Burrows-Wheeler transform (2009). Bioinformatics 25:1754–1760.

2. McKenna A, Hanna M, Banks E, et al. The Genome Analysis Toolkit: a MapReduce framework for analyzing next-generation DNA sequencing data (2010). Genome Res 20:1297–1303.

3. Wang K, Li M, Hakonarson H. ANNOVAR: functional annotation of genetic variants from high-throughput sequencing data (2010). Nucleic Acids Res 38:e164.

4. Pollard KS, Hubisz MJ, Rosenbloom KR, Siepel A. Detection of nonneutral substitution rates on mammalian phylogenies (2010). Genome Res 20:110–121.

5. Cooper GM, Stone EA, Asimenos G, Green ED, Batzoglou S, Sidow A. Distribution and intensity of constraint in mammalian genomic sequence (2005). Genome Res 15:901–913.

6. Grantham R. Amino acid difference formula to help explain protein evolution (1974). Science 185:862–864.

7. Ng PC, Henikoff S. SIFT: Predicting amino acid changes that affect protein function (2003). Nucleic Acids Res 31:3812–3814.

8. Adzhubei IA, Schmidt S, Peshkin L, et al. A method and server for predicting damaging missense mutations (2010). Nat Methods 7:248–249.

9. Schwarz JM, Cooper DN, Schuelke M, Seelow D. MutationTaster2: mutation prediction for the deep-sequencing age (2010). Nat Methods 11:361–362.